J. Cent. South Univ. (2015) 22: 409−415
DOI: 10.1007/s11771-015-2536-4

Springer

Effect of cyclic heat treatment on microstructure and mechanical properties of 50CrV4 steel

LI Hong-ying(李红英)[1], HAN Mao-sheng(韩茂盛)[1], LI De-wang(李德望)[1], LI Jun(李俊)[2], XU De-chao(徐德超)[2]

1. School of Materials Science and Engineering, Central South University, Changsha 410083, China;
2. Research Institute, Baoshan Iron & Steel Co., Ltd., Shanghai 201900, China

Abstract: An annealed 50CrV4 steel was subjected to cyclic heat treatment process that consists of repeated short-duration (200 s) held at 840 °C (above A_{c3} temperature of 790 °C) and short-duration (100 s) held at 700 °C (below A_{c1} temperature of 710 °C). The spheroidization ratio of cementite and the average size of particles increase with increasing the cyclic number of heat treatment. After 5-cycle heat treatment, the spheroidization ratio of cementite is 100%, and the average size of the cementite particles is about 0.53 μm. After cyclic heat treatment, the hardness, ultimate tensile strength and yield strength of the experimental steel gradually decrease with increasing cyclic number of heat treatment. The elongation of the as-received specimens is about 7.4%, the elongation of the 1-cycle specimen is 14.3%, and the elongation of 5-cycle specimen reaches a peak value of 22.5%, thereafter marginally decreases to 18.3% after 6-cycle heat treatment. Accordingly, the fractured surface initially exhibits the regions of wavy lamellar fracture. By increasing the cyclic number of heat treatment cycles, the regions of dimples consume the entire fractured surface gradually. Some large dimples can be found in the fracture surface of the specimen subjected to six heat treatment cycles.

Key words: cyclic heat treatment; accelerated spheroidization; mechanical properties

1 Introduction

50CrV4 steel is a kind of plate-type spring used for automotive clutch diaphragm, which has high strength, high fatigue strength and deep hardenability [1−2]. This steel is usually treated by spheroidization anneal before applying cold forming processes to obtain the spheroidized microstructure with finely distributed spherical cementite particles in a ferrite matrix. The conventional spheroidization process of steel consists of a subcritical annealing treatment that takes a long time. It requires more than 70 h of holding below the lower critical temperature (A_{c1}) for nearly 100% spheroidization [3−4]. Therefore, it has been a challenge for steel industry to reduce the time for spheroidization. In order to accelerate spheroidization, several techniques have been developed such as isothermal annealing with the aid of prior cold deformation, a combination of hot deformation and transformation of austenite to pearlite, and decomposition of supercooled austenite at a temperature slightly below Ac_1.

BARANOVA and SUKHOMLIN [5] found that under the influence of previous cold working, the process of cementite separation into piece is made easier during subcritical annealing of steel. This is mainly due to the fact that the prior cold working generates defects in the atomic crystal structure of both ferrite and cementite that affects mechanism and kinetics of pearlite spheroidization. During subcritical annealing, the cementite in worked steel is found to disintegrate along slip bands, grain, or subgrain boundaries of ferrite. By means of hot rolling and transformation of austenite to pearlite, ZHU and ZHANG [6] successfully obtained a final microstructure consisting of a ferrite matrix and spheroidization carbide particles in hypereutectoid GCr15 steel. Through a combination of low deformation temperature and slow cooling rate that happens to augment the divorced eutectoid transformation reaction, the carbide particles of experimental steel are likely to grow independently on the pre-existing carbide ‘nuclei’ and result in a poor carbon area to form ferrite. CHOU and KAO [7] found a rapid spheroidization process through the abnormal decomposition of austenite. The rapid spheroidization process is promoted by austenitizing followed by rapid quenching to a temperature slightly above the martensite-start transformation temperature (M_s), finally up-quenching to a temperature slightly below the A_{c1} temperature. The supercooled austenite possesses large dislocation density and during subcritical annealing just below A_{c1} temperature, these dislocations promote the

Received date: 2013−10−14; **Accepted date:** 2014−01−13
Corresponding author: LI Hong-ying, Professor, PhD; Tel/Fax: +86−731−88836328; E-mail: lhying@csu.edu.cn

nucleation of cementite particles and cause a rapid spheroidization finally.

In recent years, the investigations have established the potential of cyclic heat treatment techniques to accelerate cementite spheroidizing processes. SAHA et al [8−10] investigated the microstructure and mechanical properties of 0.16%, 0.6%, and 1.24% carbon steels during cyclic heat treatment. In their investigations, the spheroidization process is accelerated through short-duration at above A_{c3} temperature followed by forced air-cooling to room temperature for several cycles. The non-equilibrium temperature reversal effect during cyclic thermal treatment is explained as the prime factor causing excitation of atoms, thereby reducing the activation energy and enhancing the process kinetics. LV et al [11] also applied the cyclic heat treatment around A_1 temperature on 0.8% carbon steel and greatly accelerated the spheroidization process.

Some literatures about the spheroidization annealing of medium-carbon steel have been published [12−15], however, very few have been reported about the details of the accelerating spheriodization process in medium-carbon spring steel. The present investigation applies a cyclic heat treatment process that consists of repeated short-duration holding at the temperatures above A_{c3} and below A_{c1} in order to accelerate spheroidization process in 50CrV4 steel. The effects of cyclic numbers on the microstructure and mechanical properties of the steels are discussed.

2 Materials and experimental procedures

The as-received material used in the present investigation is annealed 50CrV4 steel sheet. The chemical composition of the steel is given in Table 1. The rectangular samples with dimensions of 150 mm× 20 mm×1.6 mm were conducted on a Gleeble-1500D thermo-mechanical simulator for a differing number of cycles, namely, 1-cycle, 3-cycle, 5-cycle and 6-cycle. Each cycle consisted of heating the specimen at 840 °C (above A_{c3} temperature of 790 °C) with the heating rate of 10 °C/s and holding for 200 s, followed by forced cooling (cooling rate of 5 °C/s) to 700 °C (below A_{c1} temperature of 710 °C) with nitrogen gas and holding for 100 s, subsequently cooling to room temperature at the speed of 10 °C/s. The schematic of the process is shown in Fig. 1(a). In order to study the extent of cementite dissolution, one as-received specimen was heated to 840 °C, held for 200 s and then quenched in water. The scheme is shown in Fig. 1(b).

Table 1 Chemical composition of 50CrV4 steel (mass fraction, %)

C	Cr	V	Si	Mn	P	S	Al	Fe
0.51	1.01	0.14	0.23	0.81	0.01	0.02	0.02	Bal.

The microstructure characteristics of as-received and heat-treated samples were examined by scanning electron microscopy (SEM) and transmission electron microscopy (TEM). The specimens for SEM observation were etched with 3% nital after mechanical polishing, and observed with a Quanta2500 scanning electronic microscope. The TEM examinations were carried out in a JET-2100F instrument, operated at 200 kV. Thin foils for TEM observation were cut by an electrical-discharge machine and mechanically ground to used discs with dimensions of d3 mm×80 μm. Then, a twin-jet electropolisher was used to produce electron-transparent thin sections in these slice discs with a solution of 5% perchloric acid and 95% ethanol at −30 °C.

The sizes of the isolated cementite spheroids were measured from SEM images. The size of a spheroid was considered as the average of major axis and minor axis of an approximated ellipse in two dimensions. At least five SEM images for each condition were examined to determine the degree of spheroidization using an image analysis program (ImageJ version 1.42). The cementite particles with the aspect ratio less than 3 were considered as spheroidal particles.

Hardness measurement was performed on a Vicker's hardness testing machine with a load of 4.9 N and an indentation time of 10 s. The tensile specimens were machined from the as-received and heat-treated samples in parallel to the rolling direction. The tensile test was conducted on a MTS810 tester at room temperature according to ISO 6892−2009. The test speed

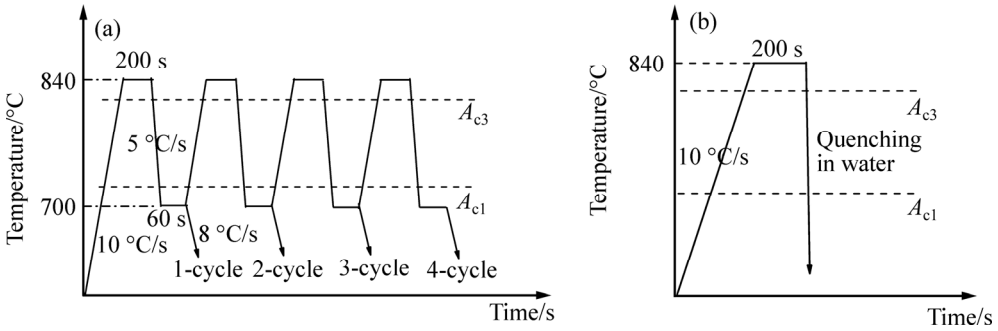

Fig. 1 Scheme of heat treatment: (a) Cyclic heat treatment; (b) Quenching in water after holding at 840 °C for 200 s

was 30 mm/min, corresponding to a strain rate of 10^{-2} s^{-1}. The morphologies of the fracture surface were observed using SEM (Quanta2500).

3 Results and discussion

3.1 Spheroidization of cementite with cyclic heat treatments

Figure 2 shows the microstructure of the as-received specimen and heat treated specimen. It can be seen that the initial microstructure is fully lamellar pearlite (Fig. 2(a)). According to Fig. 2(b), some dissolved fragmented cementite lamellae can be observed. It is indicated that the dissolution of cementite lamellae in pearlitic region remains incomplete during holding at 840 °C for 200 s. When the specimen is held at temperature above A_{c3}, austenitization starts at ferrite/cementite interface. In the process of austenitization, carbon atoms diffuse within austenite from the austenite/cementite interface to the ferrite/cementite interface owing to concentration gradient. The rate of migration of the austenite/ferrite interface is much faster than the austenite/cementite interface as the ferrite-to-austenite is a diffusionless massive polymorphic transformation. Therefore, the ferrite-to-austenite transformation occurs very fast, whereas the cementite dissolution in austenite is a slow process [16−18].

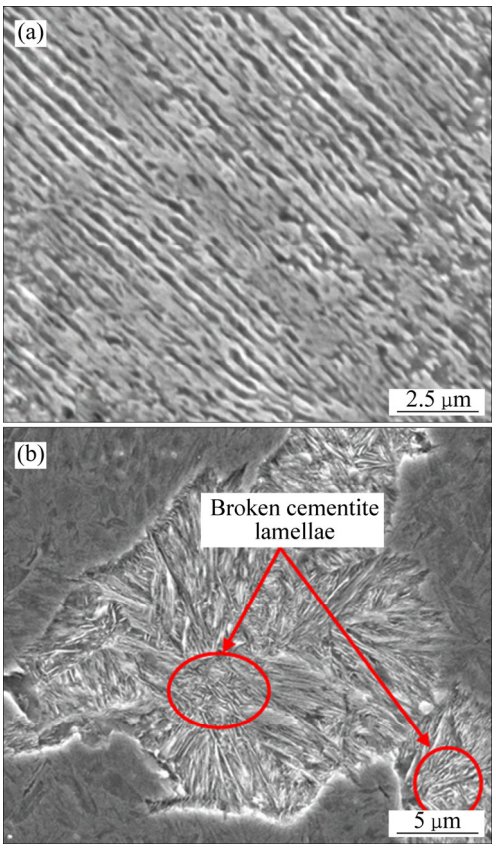

Fig. 2 SEM images of as-received specimen (a) and specimen quenched from 840 °C after holding for 200 s (b)

Figure 3 shows the TEM images of specimen subjected to heat treatment for 1-cycle. During the short time holding above A_{c3}, the cementite lattice breaks down and dissolves in austenite at the austenite/cementite interface as iron atoms join the austenite lattice and carbon atoms diffuse to the octahedral interstices of austenite. Meanwhile, the cementite lamellae are broken into fragmented lamellae, as shown in Figs. 2(b) and Fig. 3(a). When the specimen is cooled below A_{c1} temperature and held for a short time, the dissolution of cementite is terminated and the broken lamellae partially change into cementite particles. Several cementite spheroids can be found (Fig. 3(b)) at termination of lamella, which indicates that the cementite spheroids are mainly transformed from the fragmented cementite lamellae.

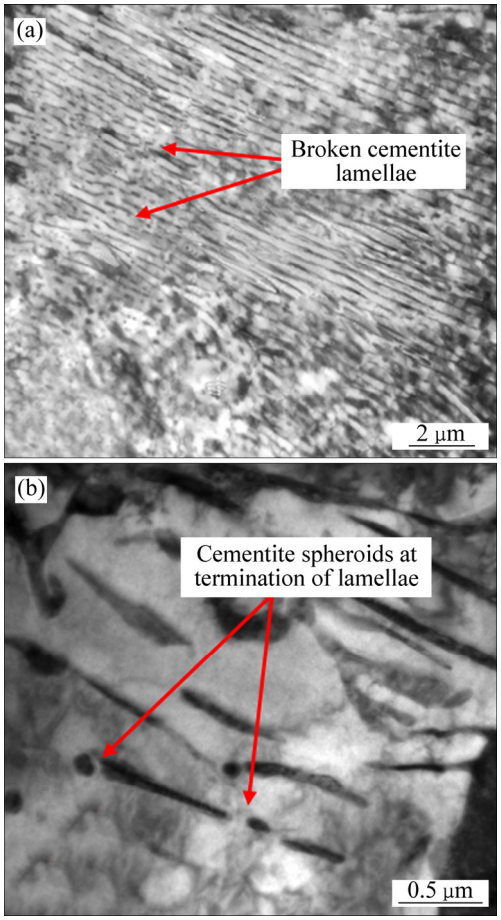

Fig. 3 TEM images of specimen subjected to heat treatment for 1-cycle: (a) Broken cementite lamellae; (b) Formation of spheroids at terminations of lamellae

Figure 4 presents the SEM images of the specimens subjected to heat treatment for different number of cycles. From Fig. 4(a), it can be seen that after 1-cycle heat treatment, only partial cementite lamellae change to cementite spheroids and the matrix mainly retains a lamellar structure. Some fragmented lamellar cementites are resulted from the incomplete dissolution of cementite

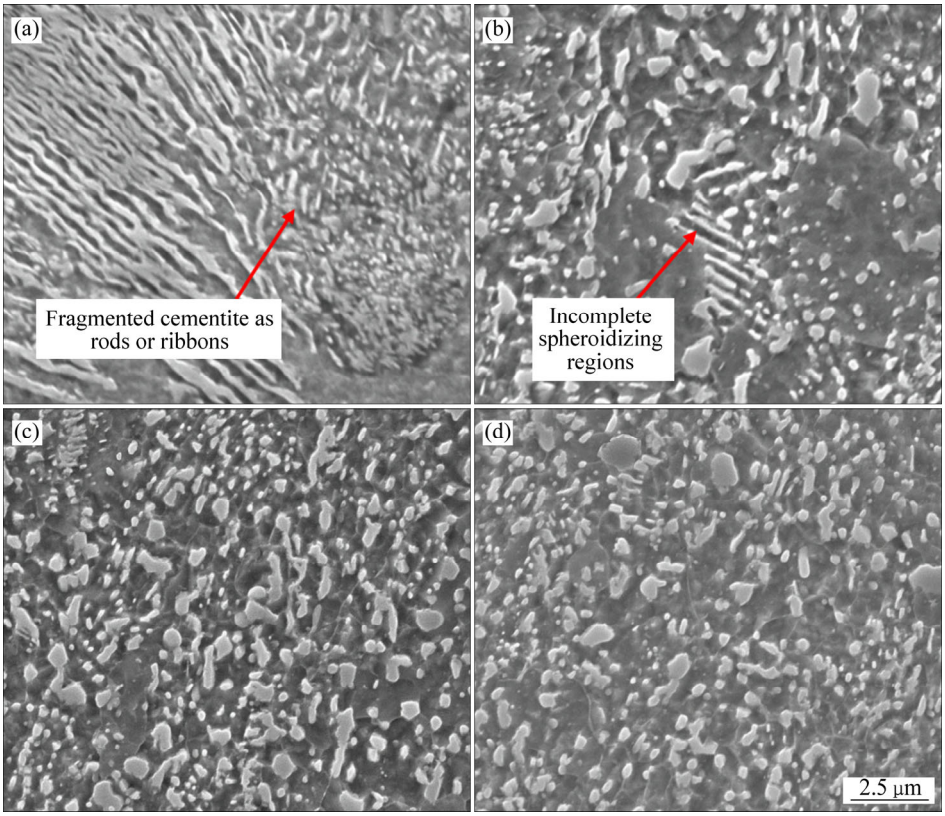

Fig. 4 SEM images of specimens subjected to heat treatment for different numbers of cycles: (a) 1 cycle, (b) 3 cycles, (c) 5 cycles; (d) 6 cycles

in form of short rods or long ribbons. By increasing cyclic numbers of heat treatment, most of the cementite lamellae are transformed to particles and the spheroidization of cementite lamellae is increased. After 3-cycle heat treatment, as seen in Fig. 4(b), only a few cementite spheroids are incomplete. According to Figs. 4(c) and (d), the microstructures consist of nearly spheroidized cementite particles. It can be concluded that the cementite spheroidizes completely after 5-cycle and 6-cycle heat treatment.

The average-size, larger particle ratio and spheroidization ratio of cementite spheroids with number of heat treatment cycles are given in Table 2. The larger particle ratio is equal to the ratio of the particle numbers of size larger than the average particle size to total statistical number. The spheroidization ratio, denoted as the ratio between volume fraction of the spherical cementite particles and the total volume fraction of all cementite particles, is measured by ImageJ from SEM images enhanced to show only carbide particles. It is difficult to calculate the spheroidization ratio after 1-cycle heat treatment due to the existence of much lamellar cementite in the microstructure. From Table 2, it can be found that the average-size, larger particle ratio and spheroidization ratio are all increased with increasing cyclic numbers of heat treatment. The average size during the 1-cycle heat treatment is the smallest, but the spheroidization ratio is the lowest. After 5-cycle heat treatment, the spheroidization ratio of cementite is 100%, and the average size of the cementite particles is about 0.53 μm.

Table 2 Rust of graphical point count analysis

Number of heat treatment cycles	Average-size/μm	Larger particle ratio/%	Spheroidization ratio/%
1	0.14	—	—
3	0.32	3.7	86
5	0.53	5.2	100
6	0.61	6.8	100

3.2. Mechanical properties

Figure 5 depicts the engineering stress−engineering strain curves from the tensile test of the experimental steel samples after different cyclic heat treatments. It can be seen that the stress−strain curves of the specimens subjected to cyclic heat treatments exhibit obvious yielding point and discontinuous yielding phenomena, compared with those of the as-received specimen (0-cycle). According to the polycrystalline yield theory, the obvious yield point is attributed to the dislocation pile-up on the ferrite grain boundaries, and dislocation activation in the ferrite grains [11, 19]. In the as-received specimen which contains lamellar pearlite structure, ferrite in the lamellar pearlite is divided by brittle and

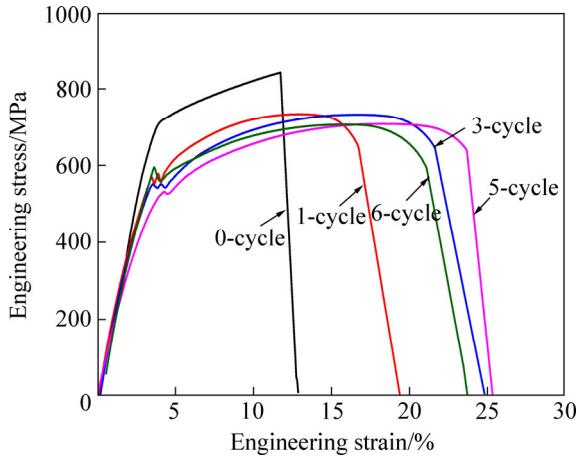

Fig. 5 Engineering stress−engineering strain curves of tensile samples after different cycles of cyclic heat treatments

hard cementite lamellae. Without multi-directional free slip-deformation, ferrite does not have the ability for cooperation-deformation. Obstacle effect of the cementite lamellae on deformation is beyond the grain boundaries. Thus, lamellar pearlite structures are unable to offer high plasticity. Correspondingly, there is no obvious yield point on the stress−strain curve. As indicated by LIN et al [20], the obvious yield point occurs as the existence of granular carbide in the grain boundary region avoids closed pearlite lamellae.

Figure 6 shows the hardness and mechanical properties (ultimate tensile strength, yield strength and elongation) of the experimental steel samples after different cyclic heat treatments. As the heat treatment cycle increase, the hardness, ultimate tensile strength and yield strength of the experimental steel gradually decrease. The ultimate tensile strength of as-received specimen (0-cycle) is about 838 MPa. After 3 heat treatment cycles, the ultimate tensile strength is 721 MPa, dropping by 14%. By increasing cyclic numbers of heat treatment, the elongation increases evidently. The elongation of as-received specimen is 7.4%, the elongation of 1-cycle specimen increases to about 14.3%, and the elongation of 5-cycle specimen reaches a peak value of 22.5%. The higher strength and lower elongation of as-received specimen are mainly due to the presence of finer microconstituents of ferrite and pearlite. After one heat treatment cycle, the marked decrease of strength and increase of elongation to failure can be attributed to the release of internal stress, the elimination of lamellar pearlite and the generation of cementite spheroids in the microstructure. The dispersed cementite particles can significantly affect the plasticity of steels. This phase was also confirmed by XIONG et al [19]. After three heat treatment cycles, the stable value of the strength and hardness of the experimental steel implies that the work-hardening effect has been eliminated and the size of the spheroidal cementite has little effect on the strength and the hardness. However, after six heat treatment cycles, the elongation marginally decreases to 18.3% with respect to that of five heat treatment cycles. This is mainly attributed to the increase of the cementite spheroids size and the larger particles ratio with increasing cyclic numbers (see Table. 2). As a consequence, the plasticity of spheroidized steel is sensitive to the larger cementite particles.

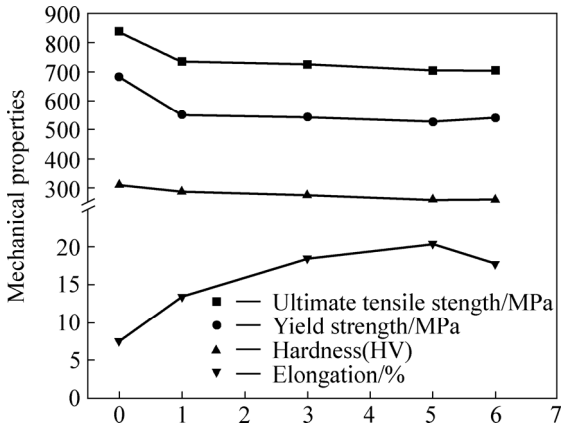

Fig. 6 Variation of hardness and mechanical properties with cyclic numbers of heat treatment

3.3 Fractured surface

The SEM images of the fractured surfaces of tensile tested specimens are presented in Fig. 7. The fractured surface of as-received steel (Fig. 7(a)) exhibits wavy regions of lamellar fracture (indicated as LF). The lamellar fracture is exhibited in the pearlitic region representing crack nucleation and propagation along the junction of different pearlite colonies. This causes poor ductility (elongation of 7.4%) of the as-received specimen. After 1-cycle heat treatment, some small dimples (indicated as D) can be found in Fig. 7(b), indicating the occurrence of the breakage and spheroidization of the cementite lamellae. Correspondingly, the ductility of the experimental steel increases to 14.3%. By increasing cyclic numbers of heat treatment, the regions of dimples gradually consume the entire fracture surface and the areas of lamellar fracture are gradually eliminated. The specimen subjected to 3-cycle heat treatment (Fig. 7(c)) exhibits dimples on majority part of the fractured surface and the pearlitic areas appear flat in a small proportion. After 5-cycle heat treatment, the entire fracture surface is occupied by dimples, as seen in Fig. 7(d). The number and depth of the dimples demonstrate the higher spheroidizing ratio of the cementite lamellae and plasticity. After 6-cycle heat treatment, some larger dimples can be found in Fig. 7(e), which are attributed to the larger cementite particles in the specimen. The microvoid coalescence mode of failure, represented by the presence of dimples, is in

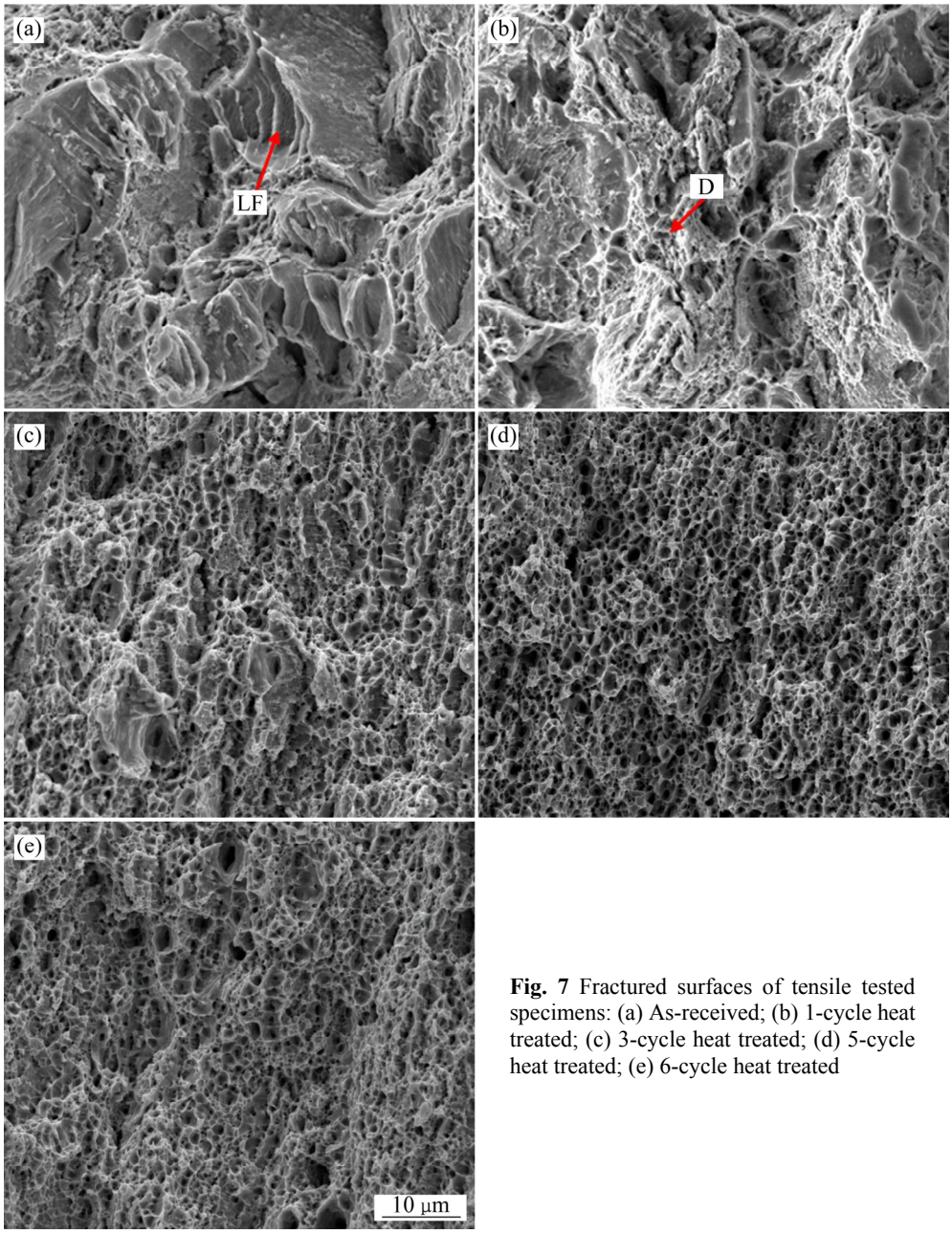

Fig. 7 Fractured surfaces of tensile tested specimens: (a) As-received; (b) 1-cycle heat treated; (c) 3-cycle heat treated; (d) 5-cycle heat treated; (e) 6-cycle heat treated

concurrence with the elimination of lamellar pearlite, and the domination of the spheroidized cementite and ferrite in the microstructure of the steel subjected to five and six cyclic heat treatments is in agreement with the microstructure of the steel in Fig. 4.

4 Conclusions

1) The cyclic heat treatment consists of repeated short duration holding at 840 °C (above A_{c3} temperature), rapid cooling to 700 °C (below A_{c1} temperature) for a short time and cooling to room temperature, which accelerates the spheroidization process of 50CrV4 steel.

2) The average size of particles and the spheroidization ratio of cementite increase with increasing cyclic numbers of heat treatment. After five cyclic heat treatments, the spheroidization ratio of cementite is 100%, the average size of the cementite particles is about 0.53 μm and the larger particles ratio is 5.2%.

3) With the increasing number of the cyclic heat treatment, the hardness, ultimate tensile strength and yield strength of the experimental steel gradually decrease and the elongation increases evidently. The elongation of 5-cycle heat treated specimen reaches a peak value of 22.5%. After six heat treatment cycles, the elongation decreases to 18.3%, which is mainly due to the increase of cementite spheroids size and the larger particle ratio with the increase of cyclic numbers.

4) The fractured surface initially exhibits the

regions of wavy lamellar fracture. The regions of dimples gradually consume the entire fracture surface and the areas of lamellar fracture are gradually eliminated with increasing cyclic numbers of heat treatment. After five cyclic heat treatments, the entire fracture surface is occupied by dimples. There are some large dimples in the fracture surface of the specimen subjected to six heat treatment cycles.

Acknowledgments

The authors are very much grateful to Research Institute, Baoshan Iron & Steel Co., Ltd., Shanghai, China, for technical assistance.

References

[1] GUO Wen-yuan, LI Jun. Subcritical spheroidization of medium-carbon 50CrV4 steel [J]. Journal of Materials Engineering and Performance, 2012, 21: 1003−1007.

[2] ÜBEYLI M, YILDIRIM R O, ÖGEL B. On the comparison of the ballistic performance of steel and laminated composite armors [J]. Materials and Design, 2007, 28: 1257−1262.

[3] MONDANL D K, DRY R M. Effect of structures on response to spheroidization in a eutectoid plain carbon steel [J]. Transactions of IIM, 1984, 37: 351−356.

[4] TIAN Yong-lai, WAYNE R K. Mechanisms of pearlite spheroidization [J]. Metallurgiacl Transaction A, 1987, 18A: 1403−1414.

[5] BARANOVA V A, SUKHOMLIN G D. Spheroidization of cementite in steel [J]. Metal Science and Heat Treatment, 1981, 11: 51−55.

[6] ZHU Guo-hui, ZHANG Gang. Directly spheroidizing during hot deformation in GCr15 steels [J]. Frontiers of Materials Science in China, 2008, 2(1), 72−75.

[7] CHOU C C, KAO P W. Accelerated spheroidization of hypoeutectoid steel by the decomposition of supercooled austenite [J]. Journal of Materials Science, 1986, 21: 3339−3344.

[8] SAHA A, MONDAL D K, BISWAS K, MAITY J. Microstructural modifications and changes in mechanical properties during cyclic heat treatment of 0.16% carbon steel [J]. Materials Science and Engineering A, 2012, 534: 465−475.

[9] SAHA A, MONDAL D K, MAITY J. Effect of cyclic heat treatment on microstructure and mechanical properties of 0.6wt% carbon steel Mater [J]. Materials Science and Engineering A, 2010, 527: 4001−4007.

[10] SAHA A, MONDAL D K, BISWAS K, MAITY J. Development of high strength ductile hypereutectoid steel by cyclic heat treatment process [J]. Materials Science and Engineering A, 2012, 541: 204−215.

[11] LV Zhi-qing, WANG Bo, WANG Zhen-hua, FU Wen-tao. Effect of cyclic heat treatments on spheroidizing behavior of cementite in high carbon steel [J]. Science and Engineering A, 2013, 574: 143−148.

[12] O'BRIEN J M, HOSFORD W F. Spheroidization of medium-carbon steels [J]. Journal of Materials Engineering and Performance, 1997, 6: 69−72.

[13] O'BRIEN J M, HOSFORD W F. Spheroidization cycles for medium carbon steels [J]. Metallurgical and Materials Transactions A, 2002, 33A: 1255−1261.

[14] KARADENIZ E. Influence of different initial microstructure on the process of spheroidization in cold forging [J]. Materials and Design, 2008, 29(1): 251−256.

[15] GANG U G, LEE J C, NAM W J. Effect of prior microstructures on the behavior of cementite particles during subcritical annealing of medium carbon steels [J]. Metals and Materials International, 2009, 15(5): 719−725.

[16] KUMAR R. Physical metallurgy of iron and steel [M]. Bombay: Asia Publishing House, 1968: 92−93.

[17] SPEICH G R, SZIRMAE A. Formation of austenite from ferrite and ferrite-carbide aggregates [J]. Transactions of the Metallurgical Society of AIME, 1969, 245: 1063−1074.

[18] SAHA A, MONDAL D K, MAITY J. An alternate approach to accelerated spheroidization in steel by cyclic annealing [J]. Journal of Materials Engineering and Performance, 2011, 20(1): 114−119.

[19] XIONG Yi, HE Tian-tian, GUO Zhi-qiang, HE Hong-yu, REN Feng-zhang, VOLINSKY A. Mechanical properties and fracture characteristics of high carbon steel after equal channel angular pressing [J]. Materials Science and Engineering A, 2013, 563: 163−167.

[20] LUO Guo-ming, WU Jing-si, FAN Jin-feng, SHI Hai-sheng, LIN Yi-jian, ZHANG Jing-guo. Microstructure and mechanical properties of spray-deposited ultra-high carbon steel after hot rolling [J]. Materials Characterization, 2004, 52(4): 263−268.

(Edited by FANG Jing-hua)